



UDC 550.42

Composition of spherules and lower mantle minerals, isotopic and geochemical characteristics of zircon from volcanoclastic facies of the Mriya lamproite pipe

Ivan G. YATSENKO¹, Sergey G. SKUBLOV², Ekaterina V. LEVASHOVA², Olga L. GALANKINA², Sergey N. BEKESHA³

¹ Institute of Geology and Geochemistry of Combustible Minerals of NAS of Ukraine, Lviv, Ukraine

² Institute of Precambrian Geology and Geochronology of RAS, Saint Petersburg, Russia

³ Ivan Franko National University of Lviv, Lviv, Ukraine

The article presents the results of studying of the pyroclastic facies of the Mriya lamproite pipe, located at Azov block of the Ukrainian shield. In them have been discovered an association of exotic mineral particles formed under super-reduce mantle conditions. These include silicate spherules, particles of native metals and intermetallic alloys, oxygen-free minerals such as diamond, qusongite (WC), and osbornite (TiN). The aim of the research is to establish the genesis of volcanoclastic rocks and to develop ideas on the highly reduced mantle mineral association (HRMMA), as well as to conduct an isotopic and geochemical study of zircon. As a result, groups of minerals from different sources are recognized in the heavy fraction: HRMMA can be attributed to the juvenile magmatic component of volcanoclastic rocks; a group of minerals and xenoliths that can be interpreted as xenogenic accidental material related to break-up of mantle nodules (hornblende, olivinite and dunite xenoliths), intrusive lamproites (tremolite-hornblende) and crystalline basement rocks (zircon, hornblende, epidote, and granitic xenoliths). The studied volcanoclastic rocks can be interpreted as intrusive pyroclastic facies (tuffisites) formed after the lamproites intrusion. Obviously, the HRMMA components formed under extreme reducing conditions at high temperatures, which are characteristic of the transitional core-mantle zone. Thus, we believe that the formation of primary metal-silicate melts of HRMMA is associated with the transition zone D".

Key words: spherules; native metals; mantle corundum; qusongite; osbornite; zircon; explosive structures; pyroclastic intrusive rocks

Acknowledgments. This study was carried out as part of the IPGG RAS research project (№ 0153-2019-0002). The authors are grateful to S.G.Simakin and E.V.Potapov (YB IPT RAS), A.N.Larionov (VSEGEI) for the analytical work, and N.T.Bilyk (University of Lviv) for the help in the result interpretation.

How to cite this article: Yatsenko I.G., Skublov S.G., Levashova E.V., Galankina O.L., Bekesha S.N. Composition of spherules and lower mantle minerals, isotopic and geochemical characteristics of zircon from volcanoclastic facies of the Mriya lamproite pipe. Journal of Mining Institute. 2020. Vol. 242, p. 150-159. DOI: 10.31897/PMI.2020.2.150

Introduction. Initially, we found an exotic association of minerals formed under extreme reducing conditions in the volcanoclastic facies of the Mriya lamproite pipe, Azov block of the Ukrainian shield. The association includes the following components: titanium-manganese-iron-silicate (TMIS) spherules, spherule-like particles of native metals and intermetallic alloys, oxygen-free minerals (diamond, moissanite, qusongite), mantle corundum with inclusions of osbornite (TiN) and Ti-Fe-Si intermetallic alloys. Further we found that various proportions of these minerals and mineral aggregates are present in the rocks of another kimberlite/lamproite structures of the Ukrainian shield, as well as in kimberlites of the Arkhangelsk and Yakutian diamondiferous provinces [8, 9, 10]. Based on the geological and geochemical data analysis, we propose the theoretical model for this mineral association formation in the transition core-mantle zone (layer D") [9], which is consistent with the concept of the layer D" composition [15]. We propose to combine all individual mineral aggregates and minerals, which are always found together and formed under similar extreme reducing conditions, into the one group namely highly reduced mantle mineral association (HRMMA). Spherules, as a product of undoubtedly endogenous processes, were first described by V.K.Marshintsev on the basis of samples findings in diamondiferous kimberlites from Yakutia [3]. A wide range of native metals (Cu, Zn, Al, Pb, Sn, Sb, Ni, and Cr) and their intermetallic alloys (Sn-Sb, Cu-Sb, and Cu-Sn) were studied in the Yakutian kimberlites by O.B.Oleinikov [4]. Mantle corundum with inclusions of osbornite (TiN), iron silicide,



and the Ti-Al-Zr compounds was first described by V.I. Tatarintsev and his colleagues in kimberlite breccias of the Western Azov region [5].

Problem statement. Over the past two decades, ideas about the fluidized explosive activity of the Earth have been actively developed. The foundations were laid in 1941 by the German geologist H. Cloos [10] based on the study of the volcanic necks of Swabia. Moreover, he introduced the term tuffisites. At present, there is no unified classification of such formations and various terms are widely used: tuffisites, intrusive pyroclastic rocks, sand tuffs, fluidolites, fluid-mud formations, pyroclastic injections. It is based on the idea of impulse (explosive) breakthrough of fluid-mineral mixtures of mantle origin. Kimberlite/lamproite structures are particular cases of a greater phenomenon of the Earth's fluidized-explosive activity. Usually, fluid-explosive rocks are a clastogenic mixture formed due to such various sources as mantle, basement rocks, and host rocks. Rocks and structures often do not have clear features indicating their deep origin, and, consequently, are interpreted as karst, glacial, impact, tectonic melange, and neptunic dikes. HRMMA is a common component of fluid-explosive formations, which can serve as a unique sign for their identification.

The aim of the research is to develop ideas of the HRMMA by the study of chemical and mineral composition of volcanoclastic rocks from the Mriya pipe. HRMMA is most fully represented in the Mriya pipe. The content of the components here is higher than in other known objects.

Geological structure. The Mriya lamproite pipe is located within the Berdyansk sub-block of the Azov block of the Ukrainian shield (Fig.1, *a, b*). Explosive structures of Konka and Kamyshy composed of lamproite-like rocks are also found here [8].

The Mriya pipe has an oval shape in the plane view with a size of 350×500 m, and goblet-shaped in the section. It is studied to a depth of over 100 m (Fig.1, *c*). The explosive structure crosses plagiogneisses and amphibolites of the Dragoonsk Unit (AR₁) of the Western Azov series. More than 100 diamond crystals were found in the so-called lamproites weathering crust of the Mriya pipe and in the overlapping alluvial deposits. The main body of the explosive structure is composed of intrusive lamproites. The main rock-forming minerals are forsterite, amphibole and phlogopite, some varieties contain clinopyroxene. The rocks are characterized by wide variations in the proportion of the main rock-forming minerals.

The object of our study was minerals from clastogenic rocks of the upper part of the pipe (with a thickness of about 20-30 m). These rocks are strongly altered with the clay-carbonate groundmass containing elliptical xenoliths. Xenoliths are 5-7 cm in size and are made of granite, micaceous hornblendite, olivinite, and dunite. Initially, these deposits were interpreted as the weathering crust of intrusive lamproites.

Research methods. Two wells with a diameter of 1300 mm were drilled in the central part of the Mriya pipe structure to study the geology of volcanoclastic deposits. The drilling rig KShK-30A was used. The initial sample volume was 500 kg. The processing was carried out at the facilities of the KP "Yuzhukrgeologiya" expedition and included the following stages: disintegration; desludging; fractionation -4 +2 mm, -2 +0.5 mm and -0.5 +0.25 mm (vibrating screen); processing on jolting machines MOD-02 and spiral classifier KR-1; drying. The final processing was carried out at the conditioning block within the Priazovskaya geological exploration crew facilities. Varieties of mineral particles were selected manually using a binocular microscope. The minerals composition was determined by the SEM-EDS at the IPGG RAS, using a JEOL JSM-6510LA scanning electron microscope with a JED-2200 energy dispersive spectrometer.

Zircon U-Pb dating was carried out at the VSEGEI Center for Isotope Research at the SHRIMP-II ion microprobe according to standard approaches [20, 22]. The data processing was conducted using special programs [17, 18]. The REE and rare elements content in zircon was determined on a Cameca IMS-4f ion microprobe in the YB IPT RAS [6, 12]. Zircon's ion microprobe analytical points coincide with previous U-Pb dating ones. The crystallization temperature of zircon

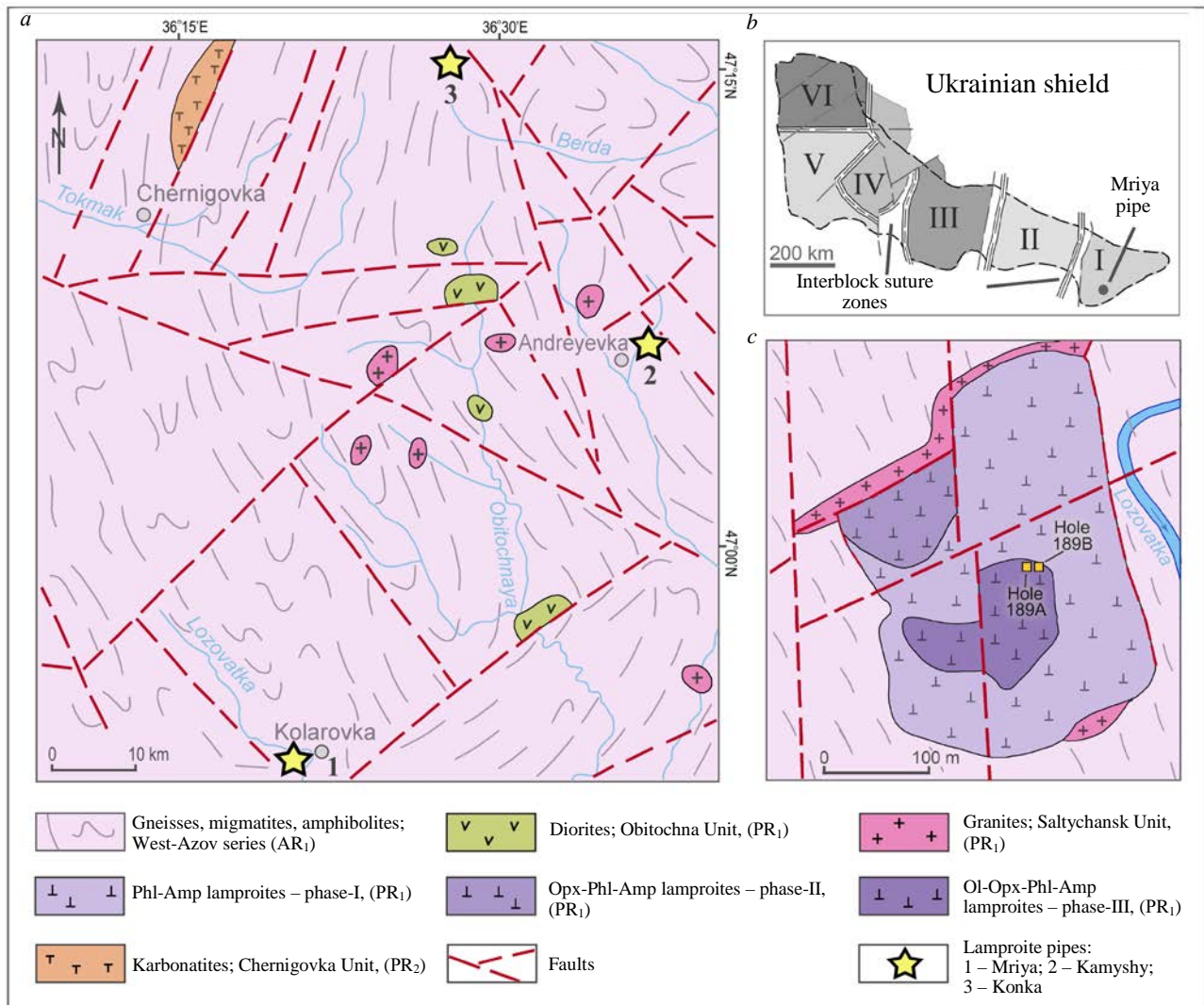


Fig.1. Location of lamproite explosive structures in the western part of the Azov block of the Ukrainian shield (a); scheme of the block structure of the Ukrainian shield (b) (I – Azov block, II – Middle-Dnieper block, III – Kirovograd block, IV – Ros-Tikich block, V – Podol block, VI – Volyn block); and the geological structure of the Mriya pipe (c) [8]

was calculated using a “Ti-in-zircon” thermometer [21]. When plotting the REE distribution spectra, the zircon composition was normalized to the composition of chondrite CI [19].

Results and discussion. We would like to present the SEM-EDS study results of the heavy mineral fraction of the volcanoclastic rocks from the Mriya pipe. The content of the heavy fraction is about 2 %. Minerals of heavy fraction can be divided into two classes: 1) a mineral suite of mantle origin (Fig.2), including TMIS spherules, particles of native metals and intermetallic alloys, mantle corundum, oxygen-free minerals (qusongite, diamond); 2) “ordinary” minerals, which can be rock-forming or accessory minerals of common types of igneous or metamorphic rocks (amphibole, plagioclase, zircon, pumpellyite, epidote, garnet, staurolite, and titanite).

Highly reduced mantle mineral association (HRMMA). The content of HRMMA components in the heavy fraction averages about 2 %.

Titanium-manganese-iron-silicate spherules are the dominant component of the HRMMA Mriya pipe. When the TMIS particles size is less than 1.5 mm, they have a spherical shape (Fig.2, a-d), if the size is larger, they acquire an irregular shape (Fig.2, e). Some particles contain a significant amount of gas bubbles (Fig.2, e). TMIS spherules may contain small spherical inclusions of native iron. In some cases, there is a crystalline phase presented by ilmenite or pyrophanite. The composition of TMIS glass is given in Table 1.



Fig.2. Microphotographs of HRMMA particles from a Mriya lamproite pipe: *a-d* – TMIS spherules; *e* – a TMIS glass particle of irregular shape; *f-r* – particles consisting of native metals and intermetallic alloys (*f-l, p* – spherule-like particles, *m-o* – particles of irregular shape, *q, r* – rod-shaped particles of native copper); *s-v* – euhedral crystals of qusongite (WC); *w-y* – grains of mantle corundum

Table 1

The major elements composition TMIS glass of Mriya pipe (wt.%)

| Analytical point number | SiO ₂ | TiO ₂ | Al ₂ O ₃ | FeO | MnO | MgO | CaO | Na ₂ O | K ₂ O | Total amount |
|-------------------------|------------------|------------------|--------------------------------|-------|-------|------|-------|-------------------|------------------|--------------|
| SH2-2-1 | 18.71 | 39.12 | 2.76 | 12.30 | 13.09 | 2.27 | 8.84 | 0.86 | 2.06 | 100.01 |
| SH2-2-2 | 19.27 | 39.87 | 2.95 | 10.25 | 12.98 | 2.44 | 9.18 | 1.07 | 1.99 | 100.00 |
| SH2-2-3 | 18.56 | 41.06 | 2.83 | 9.46 | 13.57 | 2.29 | 9.34 | 0.84 | 2.05 | 100.00 |
| SH2-2-4 | 18.49 | 39.18 | 2.84 | 12.82 | 12.86 | 2.27 | 8.97 | 0.82 | 1.75 | 100.00 |
| SH2-2-5 | 18.44 | 39.04 | 2.86 | 12.63 | 13.12 | 2.30 | 8.91 | 0.80 | 1.90 | 100.00 |
| SH2-2-6 | 18.40 | 41.91 | 3.06 | 8.77 | 13.39 | 2.37 | 9.51 | 0.80 | 1.80 | 100.01 |
| SH2-2-7 | 17.64 | 38.47 | 2.67 | 14.39 | 13.02 | 2.13 | 8.96 | 0.79 | 1.93 | 100.00 |
| VG-2012-10M | 17.87 | 39.05 | 3.69 | 16.97 | 8.98 | 1.85 | 10.93 | – | 0.66 | 100.00 |
| | 15.16 | 42.72 | 3.26 | 16.48 | 8.22 | 2.14 | 11.37 | – | 0.66 | 100.00 |
| VG-2012-17M | 17.77 | 37.99 | 2.56 | 18.68 | 11.33 | 2.80 | 8.20 | – | 1.41 | 100.74 |
| | 17.76 | 36.56 | 2.83 | 19.98 | 12.12 | 2.46 | 6.91 | – | 1.39 | 100.01 |



Particles of native metal and intermetallic alloys show a variety of shapes. Some particles have a spherical or nearly spherical shape (Fig.2, *f-l, p*), others have a completely irregular shape, often with a melted surface (Fig.2, *n, o*). Native copper particles in most cases have a cylindrical shape (Fig.2, *q, r*). According to composition, two main particles types can be distinguished: 1) particles where lead is the dominant component, with lead particles themselves and particles with different proportion of Pb, Sn, As, Sb, Ar, and Cd (Fig.2, *g-o*); 2) particles consisting of native copper (Fig.2, *p-r*). A single fragment of the Fe-Cr-Ni spherule has also been recognized (Fig.2, *f*).

Qusongite (CW) is found exclusively as individual opaque grains of steel-gray color with a bluish tint and metallic sheen, ranging from 0.2 to 2 mm in size (Fig.2, *s-v*). Commonly the mineral occurs as angular grains with irregular shape, but sub-euhedral and euhedral crystals are also found.

Mantle corundum is found as angular fragments of irregular shape with the grain size varying from 0.1 to 1.5 mm (Fig.2, *w-y*). The color of the mineral ranges from red and purple to gray and brown. A characteristic feature of the mineral is the presence of oxygen-free phase inclusions, as well as amorphous oxide and crystalline oxide phases. Another mantle corundum feature is the constant presence of titanium impurities in the content of up to 2 wt.%. The inclusions of oxygen-free phases are represented by osbornite (TiN) and Ti-Fe silicides (Table 2).

Table 2

The composition of oxygen-free phases inclusions in mantle corundum (wt.%)

| Analytical point number | Alloy components | Si | Ti | Al | Cr | Fe | Mn | Mg | Ca | Cu | K | P | S | total amount |
|-------------------------|------------------|-------|-------|------|------|-------|------|------|------|------|------|------|-------|--------------|
| Cr3-1-2-1 | Wassonite (TiS) | 2.50 | 51.48 | 3.05 | – | – | 1.77 | 0.26 | 2.18 | – | – | – | 38.76 | 100.00 |
| Cr3-1-2-1 | (TiS) | 2.30 | 53.14 | 1.83 | – | – | 1.38 | – | 1.49 | 0.58 | 0.24 | – | 39.04 | 100.00 |
| Cr3-1-2-2 | Fe-Ti-Si | 21.21 | 25.79 | 0.62 | 2.63 | 47.72 | 2.03 | – | – | – | – | – | – | 100.00 |
| Cr3-1-3 | Fe-Si | 15.37 | 4.33 | – | 1.75 | 78.50 | 0.05 | – | – | – | – | – | – | 100.00 |
| Cr3-1-3 | Fe-Si | 15.99 | 5.03 | – | 1.81 | 77.17 | – | – | – | – | – | – | – | 100.00 |
| Cr3-1-3 | Fe-Ti-Si | 20.31 | 29.41 | – | 1.87 | 48.03 | 0.39 | – | – | – | – | – | – | 100.01 |
| Cr3-1-3 | Fe-Ti-Si | 20.01 | 28.38 | – | 2.09 | 49.17 | 0.35 | – | – | – | – | – | – | 100.00 |
| Cr3-1-3 | Fe-Si | 23.02 | 6.90 | – | 2.24 | 67.56 | 0.29 | – | – | – | – | – | – | 100.01 |
| Cr3-1-3 | Fe-Si | 22.49 | 6.52 | – | 2.31 | 68.42 | 0.26 | – | – | – | – | – | – | 100.00 |
| Cr3-1-4 | Fe-Si | 16.28 | 4.00 | – | 1.53 | 78.19 | – | – | – | – | – | – | – | 100.00 |
| Cr3-1-4 | Fe-Ti-Si | 19.25 | 29.41 | – | 1.12 | 48.96 | – | – | – | – | – | 1.27 | – | 100.01 |

Among the oxide inclusions in mantle corundum, five main types can be distinguished: Ti-Zr-Al and Ti-Al amorphous phases with a rather variable composition; crystalline phase represented by hibonite; rutile and feldspar (in particular, andesine) phases.

Diamond shows cuboctahedral crystals 0.1-0.3 mm in size. Diamonds are well preserved (safety factor is 2.5), semitransparent, with yellow, yellow-green, and gray-green color.

Rock-forming and accessory minerals of common rock types. Obviously, while HRMMA can be assigned to the juvenile magmatic components of the volcanoclastic facies from the Mriya pipe, rock-forming and accessory minerals can be interpreted as accidental material related to the destruction mantle nodules, intrusive lamproites, and crystalline basement rocks. The major components of the heavy mineral fraction (about 80 %) are amphiboles, zircon and rounded grains, consisting of a cryptocrystalline aggregate, including barite, actinolite, and dolomite. The rest of the components contains ilmenite, plagioclase, pumpellyite, epidote, garnet, staurolite, titanite, and components of HRMMA in various proportions.

There are two varieties of amphiboles. The first one is calcium amphiboles, more specifically, tremolite-hornblende series, transparent and green colored minerals with empirical formula $(\text{Na}_{0.05}\text{K}_{0.04})_{0.09}(\text{Ca}_{1.80}\text{Na}_{0.19})_{2.00}(\text{Mg}_{4.13}\text{Fe}^{2+}_{0.87}\text{Mn}_{0.08}\text{Al}_{0.06})_{5.14}[(\text{Si}_{7.78}\text{Al}_{0.22})_{8.00}\text{O}_{22}](\text{OH})_2$; The second variety is a black hornblende with empirical formula $(\text{Na}_{0.36}\text{K}_{0.25})_{0.61}(\text{Ca}_{1.99}\text{Na}_{0.01})_{2.00}(\text{Mg}_{2.30}\text{Fe}^{2+}_{2.19}\text{Al}_{0.48}\text{Ti}_{0.08}\text{Mn}_{0.04})_{5.09}[(\text{Si}_{6.60}\text{Al}_{1.40})_{8.80}\text{O}_{22}](\text{OH})_2$. The composition of the first amphiboles type corresponds to the amphiboles of the intrusive lamproites of the Mriya pipe and, thus,



they can be probably the product of the earlier intrusive phases destruction. The hornblende of the second type does not correspond to the known amphibole species from intrusive lamproites and, presumably, is associated with the destruction of metamorphic rocks of the crystalline basement.

Garnet is presented by two varieties: pink almandine-pyropite with empirical formula $(\text{Fe}^{2+}_{2.34}\text{Mg}_{0.48}\text{Ca}_{0.17}\text{Mn}_{0.05})_{3.05}(\text{Al}_{1.87}\text{Fe}^{3+}_{0.12})_{1.99}[\text{Si}_{2.97}\text{O}_{12}]$ and reddish-brown andradite-grossular $(\text{Ca}_{2.92}\text{Mg}_{0.08})_3(\text{Al}_{1.09}\text{Fe}^{3+}_{0.87})_{1.95}[\text{Si}_{3.02}\text{O}_{12}]$.

The fragments of plagioclase-epidote-bearing rock are most likely xenogenic, formed due to the metamorphic basement rocks destruction, the empirical formula of epidote is $\text{Ca}_{2.03}(\text{Fe}^{3+}_{0.89}\text{Mg}_{0.09}\text{Mn}_{0.01})_{0.99}\text{Al}_{1.90}[\text{Si}_{3.08}\text{O}_{11}]\text{O}(\text{OH})$. Plagioclase has andesine composition.

Pumpellyite is found in the form of olive-colored rounded transparent grains with the empirical formula $\text{Ca}_{1.90}(\text{Fe}^{2+}_{0.62}\text{Al}_{0.37})\text{Al}_{2.00}[\text{Si}_{2.96}\text{O}_{11}](\text{OH})_2 \cdot \text{H}_2\text{O}$.

Staurolite is presented by red-brown rounded transparent grains with the empirical formula $(\text{Fe}^{2+}_{1.42}\text{Mg}_{0.50})_{1.92}(\text{Al}_{8.54}\text{Fe}^{3+}_{0.42})_{8.96}[\text{Si}_{3.39}\text{O}_{20}](\text{O}, \text{OH})_4$.

Titanite forms euhedral grains of brownish colors of up to 1 mm in size.

Microcrystalline barite-actinolite-dolomite aggregate forms rounded white grains. Grain size is up to 2 mm. The formation of these particles can be related to the secondary alteration processes.

Zircon. The size of the studied zircon reaches 400-500 μm . Zircon is presented by moderately rounded crystals or their fragments (Fig.3, *a*). Most of zircon grains has a dark, even black, hue in the CL images, with traces of banded growth oscillatory zonation. In some cases, mosaic zonation, combined with oscillatory one (grains 10.1, 12.1, 13.1) is observed. Some zircon grains have rims visible in CL due to the dark gray or, less commonly, white hue. Some zircon grains are characterized by thin-banded growth zonation, revealed due to the gray tones in the CL images (for example, grains 6.1, 7.1, 15.1).

The zircon crystal from a rounded domain, characterized by the black color and no zonation in CL image and located inside a grain with a thin-band oscillatory zonation (point 13.1, Fig.3, *a*), shows the most ancient sub-concordant $^{207}\text{Pb}/^{206}\text{Pb}$ age of 3728 ± 12 Ma. This domain is characterized by the highest, among the studied zircon, U content of 325 ppm, and Th/U ratio of 0.79. The rest of the analyzed zircon points form a sub-concordant cluster in the concordia diagram (Fig.3, *b*). The three zircon points (6.1, 11.1, and 7.1, Fig.3, *a*) differ from other points in the cluster by the more ancient value of $^{207}\text{Pb}/^{206}\text{Pb}$ age, falling in the 3022-3060 Ma interval. The CL image of these points shows dark gray hue and thin-band oscillatory zoning. The U content at these points is 38-87 ppm (much lower than at point 13.1) with the Th/U ratio of 0.24-0.47. The discordia with a value of the upper intersection of 2909 ± 13 Ma can be driven through 9 points (Fig.3, *b*). The intersection can be considered as the crystallization age of this zircon. The value of the lower discordia intersection of 595 ± 680 Ma corresponds to the beginning of concordia and can be interpreted as the loss of radiogenic Pb in modern times. The content of Th and U in the zircon understudy varies from the first tens to 300 ppm, the Th/U ratio ranges from 0.62 to 3.10, averaging 1.18, which is typical for magmatic zircon [13]. The entire studied zircon grains show a similar REE distribution (Fig.3, *c*) with high fractionation from LREE to HREE (the Lu_N/La_N average value is 6068), clearly pronounced positive Ce-anomaly (the Ce/Ce^* average value is 63) and negative Eu-anomaly (Eu/Eu^* averages 0.38). The total REE content varies from 213 to 1241 ppm, correlating with the content of Y and P. The minimum content of Y, P, and REE was revealed in zircon with the highest $^{207}\text{Pb}/^{206}\text{Pb}$ age (points 13.1, 6.1, 11.1, and 7.1). These points are characterized by a lower Hf content. Most likely, the ancient zircon origins from the basic rocks [14]. At other zircon analytical points, the Y content can be five times higher, and the content of Hf and P also increases. Such geochemical characteristics are common to the zircon from granitoids and intermediate rocks.

The content of elements, not included in the mineral formula: Ca, Sr, and Ba is low, which indicates the absence of zircon under the fluids driven alteration processes. According to the "Ti-in zircon" thermometer [11] the temperature value falls within the range of 640-870 °C with

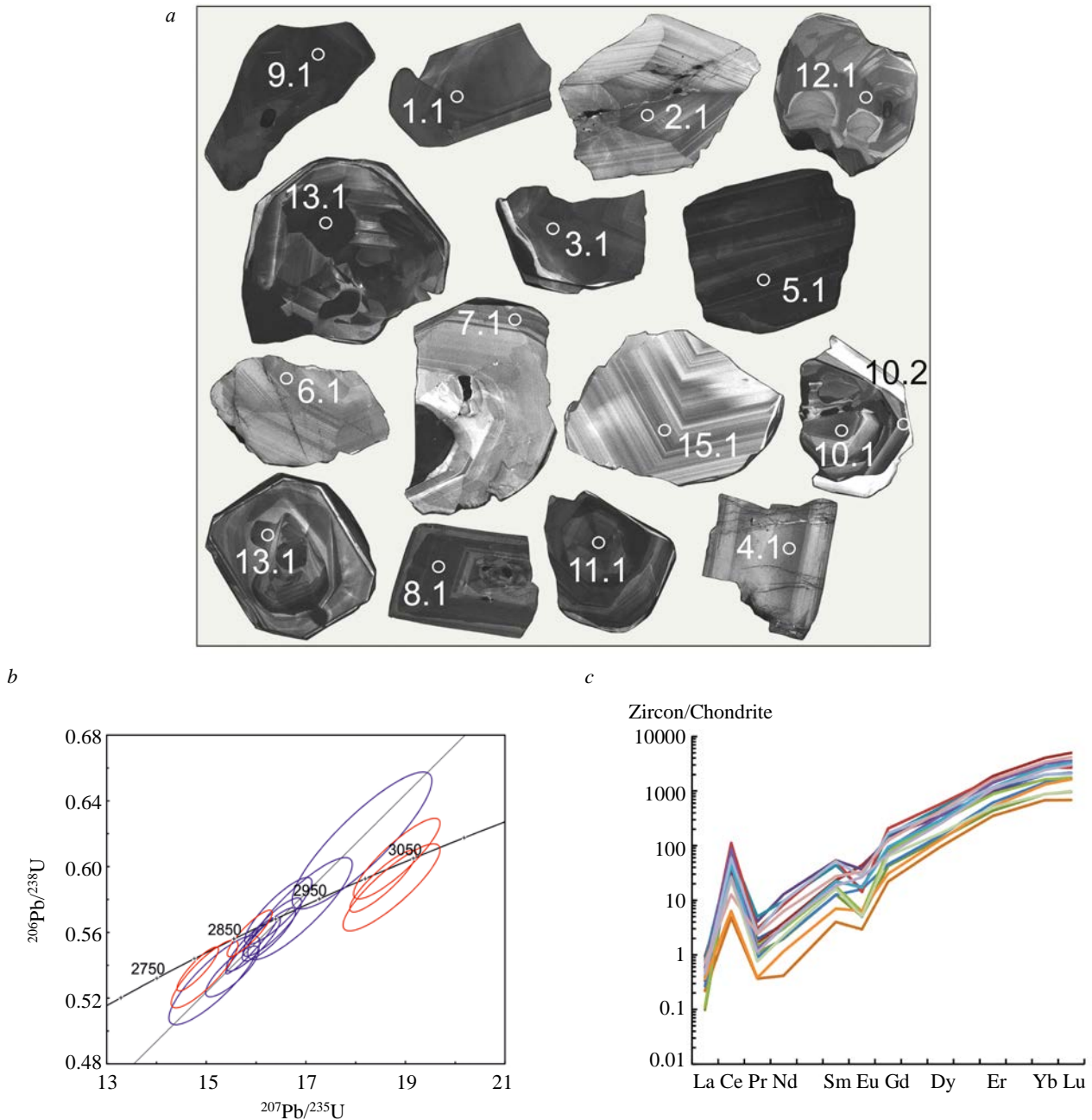


Fig.3. CL-images of zircon from the Mriya pipe, the size of the ion microprobe crater is about 20 μm (a); concordia diagram for zircon from the Mriya pipe (b); REE spectra in zircon from the Mriya pipe (c)

an average value of 715 $^{\circ}\text{C}$. These temperature values can be considered as crystallization conditions of magmatic zircon, or as parameters of granulite metamorphism superimposed on magmatic zircon.

Earlier, zircon and phlogopite from micaceous ultrabasites of the Mriya pipe have shown the age of 2000-1720 Ma, taken as the age of the pipe's rocks formation [1]. The vein body of aplite-like granites, intersecting micaceous ultrabasites of the Mriya pipe, has an age of 1720 ± 20 Ma [7]. It is reasonable to assume that the studied zircon is xenogenic for pipe rocks and was captured during its intrusion from the basement rocks. According to the geological data, the pipe rocks break through the migmatized plagiogneisses and amphibolites of the Paleoproterozoic Dragoonsk Unit. Geochronological data for rocks of the Dragoonsk Unit are very limited. There is the only one published data on the $^{207}\text{Pb}/^{206}\text{Pb}$ dating of zircon single fraction from garnet-biotite gneiss with the determined age of about 3054 Ma [2].



The formation of gabbro and granitoid intrusions show a relatively narrow time interval of 2940-2910 Ma. This data was obtained via the in-situ dating of zircon from various rocks of the Saltychansk igneous province, hosting the Mriya pipe [16]. The zircon age values, presented in this work (2909 ± 13 Ma, Fig.3, *b*) coincide with these data within the accuracy. Noticeable differences in rare elements (P, Y, Hf) content suggest that zircon was captured from approximately even-aged rocks of different composition – gabbro and granitoids. A single find of older zircon with $^{207}\text{Pb}/^{206}\text{Pb}$ age of 3728 ± 12 Ma indicates the presence of Paleoarchean rocks in the lower part of the basement. It is assumed that dunites occurring among the Mriya pipe's rocks were formed in intermediate magma chambers at great depths [8] and, when moving to higher levels, they captured zircon from rocks of the lower basement level.

In previous studies of the Mriya pipe, the rocks of the volcanoclastic facies were interpreted as the weathering crust of intrusive lamproites. Our research has shown that the rocks mineral fraction is xenogenic with respect to intrusive lamproites. All components except tremolite-hornblende series can be attributed to accidental material with different sources, entrained during explosive intrusion. Based on the expected sources of the mineral particles, the following mineral associations can be distinguished: 1) juvenile mineral particles of mantle origin, including TMIS spherules, particles of native metals and intermetallic alloys, mantle corundum, oxygen-free minerals (qusongite, diamond); 2) hornblendite, olivinite and dunite xenoliths associated with the disintegration of mantle nodules; 3) tremolite-hornblende grains, probably entrained from intrusive lamproites; 4) accidental material related to igneous and metamorphic rocks of the crystalline basement and including the following components: zircon, black hornblende, plagioclase, epidote and granite xenoliths; 5) secondary minerals represented by clay and carbonate groundmass minerals, as well as numerous barite-actinolite-dolomite aggregates; 6) minerals of undetermined origin, such as garnets, staurolite, titanite (on the one hand, they can be fragments of crystalline basement rocks, on the other hand, observations have shown that they usually occur together with HRMMA in various rocks, i.e. may be of mantle origin).

Based on the results the mineral composition studies, we believe that the studied rocks are not the weathering crust of the intrusive lamproites, but are an individual intrusive pyroclastic or tuffisite facies of the Mriya pipe, intruded after the formation of the intrusive lamproites bodies. This statement is important for understanding the prospects for the Mriya pipe's diamond potential. According to the generally accepted model of the Mriya pipe structure, the facies considered by us as volcanoclastic compose the upper part of the structure with a thickness of several tens of meters and overlap the intrusive facies (see Fig.1, *c*). According to the unpublished data of S.N.Strekozov, the distribution of facies in the pipe's section is much more complex in comparison with the known model. Drilling data show an unstable alternation of intrusive lamproites, host rocks and crushing zones. Thus, it is possible that the pipe's main body has a block structure similar to block breccias with veining intrusive pyroclastites that form a stockwork structure.

The experience of HRMMA study in explosive structures of various diamondiferous provinces shows that all the components are found exclusively as individual formations, showing no affinity for either host explosive rocks or deep xenoliths (Iherzolites, eclogites). In other words, each particle is an individual “magmatic” system formed in a fluid environment with a sharp cooling, i.e. under conditions inconsistent with those generally accepted for the igneous rocks formation. The question that has to be answered is what are the primary sources of silicate-metal spherules? Obviously, the initial HRMMA melts were formed under extreme reducing conditions at extremely high temperatures [9]. A stable large-scale occurrence of such conditions with the equilibrium presence of refractory silicate, oxide, and metal phases can be expected only in the transition core-mantle zone. It can be assumed that the formation of primary metal-silicate HRMMA melts is associated with the transition D" zone [9, 11]. These conclusions are consistent with the F.V.Kaminsky's concept on the compositional characteristics of lower mantle and transitional core-mantle zone[15].



Conclusions

1. We have revealed that the studied volcanoclastic deposits of the Mriya pipe cannot be the lamproites weathering crust. We interpret them as intrusive pyroclastic facies (tuffisites) formed after the lamproites intrusion.

2. Intrusive pyroclastic rocks consist of juvenile components of mantle origin (HRMMA), mantle xenoliths of ultrabasic rocks, xenogenic accidental material related to the host rocks and secondary minerals. It should be noted that diamonds were discovered right in these Mriya pipe's rocks.

3. The stable trend of the HRMMA components to form spherical shapes indicates that they were formed directly from the melt as a result of its sputtering in fluid flows.

4. The key observation is that the HRMMA components are found together, but do not show any relationships to each other, nor do they show an affinity for known mantle rocks. It is likely that the HRMMA source were isolated volumes of the corresponding melts located in the transition core-mantle zone. One should not consider the existence of such melts as an exotic phenomenon associated with kimberlite or lamproite magmatism; rather, it is a global phenomenon. The analysis showed that the HRMMA particles findings are not necessarily associated with a specific rock type [3, 4, 9], but are rather related to the various explosive structures and the volcanoclastic facies of these structures in particular.

REFERENCES

1. Artemenko G.V., Bartnitskii E.N., Dovbush T.I., Ponomarenko A.N., Stepanyuk L.M. The age of micaceous ultrabasites of the Mriya pipe. Azov block. *Mineralogicheskii zhurnal*. 1999. Vol. 21. N 2/3, p. 76-78 (in Russian).
2. Artemenko G.V., Shvaika I.A., Demedyuk V.V., Dovbush T.I., Vysotskii A.B. Age and genesis of metamorphic rocks of the Dragoonsk sequence in the western part of the Belotserkovska structure (Azov block). *Mineralogicheskii zhurnal*. 2012. Vol. 34. N 1, p. 69-75 (in Russian).
3. Marshintsev V.K. The nature of spheroid formations in kimberlites. In the book: Traces of cosmic influences on the Earth. Novosibirsk: Nauka, 1990, p. 45-57 (in Russian).
4. Oleinikov O.B. Native metals in eclogites from the Obnazhennaya pipe. In the book: Native metals in igneous rocks. Yakutsk, 1985, p. 72-73 (in Russian).
5. Tatarintsev V.I., Tsimbal S.N., Sandomirskaya S.M. The first finding of titanium nitride (osbornite) in the Earth rocks. *Doklady AN SSSR*. 1987. Vol. 296. N 6, p. 1458-1461 (in Russian).
6. Fedotova A.A., Bibikova E.V., Simakin S.G. Zircon geochemistry (ion microprobe data) as an indicator of its genesis in geochronological studies. *Geochemistry International*. 2008. Vol. 46. N 9, p. 912-927.
7. Shcherbak N.P., Ponomarenko A.N., Lesnaya I.M. Comparative geochronology of rock associations and ore formations of the Proterozoic eon (2.5-1.6 Ga) of the Ukrainian shield megablocks. *Mineralogicheskii zhurnal*. 2012. Vol. 34. N 3, p. 45-54 (in Russian).
8. Yatsenko G.M., Bekesha S.N., Gaiovskii O.V., Yatsenko I.G. Activation periods, ore-bearing structures and formations of the lamproite type in the Archean and Proterozoic blocks of the Ukrainian shield. Article 1. West Azov block. *Mineralni resursi Ukraini*. 2011. 2010. N 4, 27-32 (in Russian).
9. Yatsenko I.G. Silicate-metal spheres of explosive-sedimentary formations of Ukraine (genetic and prospecting aspects): Theses. kand. geol. nauk / Lvovskii natsionalnyi universitet imeni Ivana Franko. Lvov, 2016, p. 29. (in Ukrainian)
10. Cloos H. Bau und Taetigkeit von Tuffschloten. *Geologische Rundschau*. 1941. Vol. 32. Iss. 6-8, p. 708-800.
11. Yatsenko I.G., Zinchenko V.N., Marshyntsev V.K., Bekesha S.N., Bilyk N.T. *Materialy yubileinogo sezda Rossiiskogo mineralogicheskogo obshchestva "200 let RMO"*. Vol. 1. St. Petersburg, 2017, p. 361-363.
12. Hinton R.W., Upton B.G.J. The chemistry of zircon: variations within and between large crystals from syenite and alkali basalt xenoliths. *Geochimica et Cosmochimica Acta*. 1991. Vol. 55 (32), p. 3287-3302.
13. Hoskin P.W., Schaltegger U. The composition of zircon and igneous and metamorphic petrogenesis. *Reviews in Mineralogy and Geochemistry*. 2003. Vol. 53, p. 27-62.
14. Belousova E.A., Griffin W.L., O'Reilly S.Y., Fisher N.I. Igneous zircon: trace element composition as an indicator of source rock type. *Contributions to Mineralogy and Petrology*. 2002. Vol. 143, p. 602-622.
15. Kaminsky F.V. The Earth's Lower Mantle. Composition and Structure. Cham: Springer Geology, 2017, p. 331.
16. Bibikova E.V., Lobach-Zhuchenko S.B., Artemenko G.V., Claesson S., Kovalenko A.V., Krylov I.N. Late Archean magmatic complexes of the Azov terrane, Ukrainian Shield: Geological setting, isotopic age, and sources of material. *Petrology*. 2008. Vol. 16, p. 211-231.
17. Ludwig K.R. SQUID 1.02, a User Manual, a geochronological toolkit for Microsoft Excel. Berkeley: Berkeley Geochronology Center, Special Publication, 2001, p. 19.



18. Ludwig K.R. Users manual for Isoplot/Ex version 3.0: a geochronological toolkit for Microsoft Excel. Berkeley: Berkeley Geochronology Centre, Special Publication, 2003, p. 74.
19. McDonough W.F., Sun S.S. The composition of the Earth. *Chemical Geology*. 1995. Vol. 120, p. 223-253.
20. Black L.P., Kamo S.L., Allen C.M., Aleinikoff J.N., Davis D.W., Korsch R.J., Foudoulis C. TEMORA 1: a new zircon standard for Phanerozoic U-Pb geochronology. *Chemical Geology*. 2003. Vol. 200, p. 155-170.
21. Watson E.B., Wark D.A., Thomas J.B. Crystallization thermometers for zircon and rutile. *Contribution to Mineralogy and Petrology*. 2006. Vol. 151, p. 413-433.
22. Williams I.S. U-Th-Pb geochronology by ion microprobe. In: Applications of microanalytical techniques to understanding mineralizing processes. *Reviews in Economic Geology*. 1998. Vol. 7, p. 1-35.

Authors: Ivan G. Yatsenko, Candidate of Geological Sciences, Senior Researcher, yatsenko.ivan1000@gmail.com (Institute of Geology and Geochemistry of Combustible Minerals of NAS, Lviv, Ukraine), Sergey G. Skublov, Doctor of Geological and Mineralogical Sciences, Chief Researcher, skublov@yandex.ru (Institute of Precambrian Geology and Geochronology RAS, Saint Petersburg, Russia), Ekaterina V. Levashova, Candidate of Geological and Mineralogical Sciences, Junior Researcher, levashova.kateryna@yandex.ru (Institute of Precambrian Geology and Geochronology RAS, Saint Petersburg, Russia), Olga L. Galankina, Candidate of Geological and Mineralogical Sciences, Senior Researcher, galankinaol@mail.ru (Institute of Precambrian Geology and Geochronology RAS, Saint Petersburg, Russia), Sergey N. Bekesha, Candidate of Geological and Mineralogical Sciences, Associate Professor, smbekesha@ukr.net (Ivan Franko National University of Lviv, Lviv, Ukraine).

The paper was received on 4 September, 2019.

The paper was accepted for publication on 18 December, 2019.